

Research Article

Maximum SINR Synchronization Strategies in Multiuser Filter Bank Schemes

Francesco Pecile and Andrea M. Tonello (EURASIP Member)

*Dipartimento di Ingegneria Elettrica Gestionale e Meccanica (DIEGM), Università di Udine,
Via delle Scienze 208–33100 Udine, Italy*

Correspondence should be addressed to Andrea M. Tonello, tonello@uniud.it

Received 23 November 2009; Revised 11 June 2010; Accepted 21 July 2010

Academic Editor: Carles Anton-Haro

Copyright © 2010 F. Pecile and A. M. Tonello. This is an open access article distributed under the Creative Commons Attribution License, which permits unrestricted use, distribution, and reproduction in any medium, provided the original work is properly cited.

We consider synchronization in a multiuser filter bank uplink system with single-user detection. Perfect user synchronization is not the optimal choice as the intuition would suggest. To maximize performance the synchronization parameters have to be chosen to maximize the signal-to-interference-plus-noise ratio (SINR) at each equalizer subchannel output. However, the resulting filter bank receiver structure becomes complex. Therefore, we consider two simplified synchronization metrics that are based on the maximization of the average SINR of a given user or the aggregate SINR of all users. Furthermore, a relaxation of the aggregate SINR metric allows implementing an efficient multiuser analysis filter bank. This receiver deploys two fractionally spaced analysis stages. Each analysis stage is efficiently implemented via a polyphase filter bank, followed by an extended discrete Fourier transform that allows the user frequency offsets to be partly compensated. Then, sub-channel maximum SINR equalization is used. We discuss the application of the proposed solution to Orthogonal Frequency Division Multiple Access (OFDMA) and multiuser Filtered Multitone (FMT) systems.

1. Introduction

In this paper, we consider the asynchronous multiple access wireless channel (uplink) where the devices transmit signals that experience different carrier frequency offsets, propagation delays, and propagate through independent frequency selective fading channels. In particular, we consider the use of filter bank modulation (FBM) combined with frequency division user multiplexing, that is, with the allocation of the available subchannels among the users [1]. In FBM, a high data rate signal is transmitted through parallel narrow band subchannels that are shaped with a prototype pulse. Two significant examples are Orthogonal Frequency Division Multiplexing (OFDM) [2] and Filtered Multitone Modulation (FMT) [3]. The former scheme privileges the time confinement of the subchannels since it deploys rectangular impulse response subchannel pulses. The latter privileges the frequency domain confinement since it deploys frequency confined pulses. Both schemes enjoy an efficient implementation based on a fast Fourier transform (IFFT). In FMT, low-rate subchannel filtering has also to be deployed [3, 4].

Synchronization in OFDM and multiuser OFDM (OFDMA) has received great attention and several results have been obtained, for example, the algorithms in [5–10]. On the contrary synchronization in FMT systems, and more in general in multiuser FMT, has not been extensively investigated. Synchronization involves the estimation of the users time and frequency offsets that are different among the users in the uplink. In [11], a nondata-aided timing recovery scheme has been proposed for single-user FBM. Recently, we have analyzed in [12] the synchronization problem for multiuser FMT, and we have proposed data-aided correlation metrics that aim at obtaining perfect synchronization with each user. In this paper we bring new insights and we investigate how the synchronization metric impacts the complexity and performance in multiuser FBM. We assume the deployment of single-user detection which consists in the acquisition of time and frequency synchronization with the user of interest followed by subchannel equalization. The intuition suggests that the receiver has to be perfectly time- and frequency-synchronized to the user of interest. Single-user detection architectures with perfect synchronization in

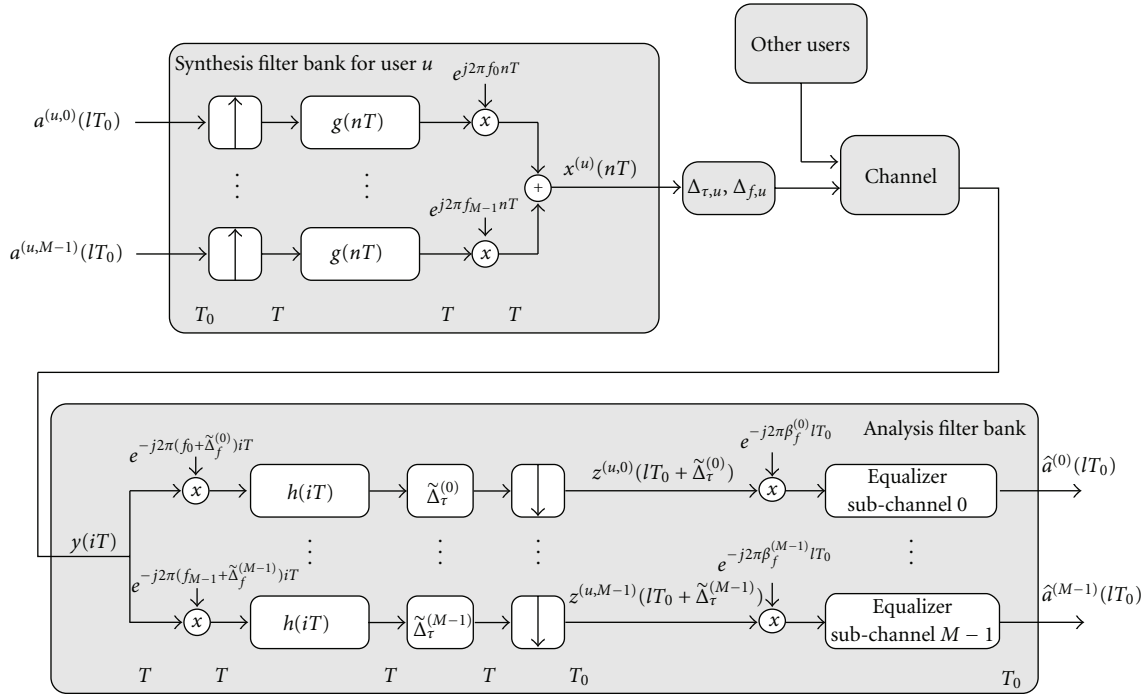


FIGURE 1: Filter bank system model with time/frequency compensation at subchannel level.

multiuser OFDM (OFDMA) have been considered in [6–10]. The idea of achieving perfect compensation of the carrier and time offsets in multiuser FMT has been also applied for the development of the synchronization metrics in [12].

However, perfect synchronization is not the optimal choice. In fact, in the uplink each user experiences its own channel, time offset, and carrier frequency offset. Thus, the receiver may suffer of the presence of multiple access interference (MAI), as well as intercarrier interference (ICI) and intersymbol interference (ISI) [1, 6–8]. To maximize performance the synchronization parameters have to be chosen to maximize the signal-to-interference-plus-noise ratio (SINR) at the detection point in each subchannel. We show that it is possible to implement different receiver filter bank (FB) structures depending on the specific SINR criterion adopted, which leads to the use of

- a subchannel synchronized filter bank if the goal is to maximize the subchannel SINR,
- a user synchronized filter bank if the goal is to maximize a user-defined SINR,
- a single filter bank for all users if the goal is to maximize an aggregate SINR,
- a fractionally spaced filter bank with partial compensation of the carrier frequency offsets.

All these receivers deploy maximum SINR subchannel equalization to deal with the subchannel ISI. Although the receiver (a) is optimal, it suffers of high complexity because it needs to run an exhaustive search of the optimal parameters to compensate the time and frequency offset for

each subchannel. Furthermore, the implementation of the analysis filter bank cannot exploit the efficient polyphase discrete Fourier transform (DFT) filter bank realizations described in [3, 4] that require a common sampling phase for all the subchannels. Lower complexity is obtained with the receiver (b) and (c), although the synchronization metric still requires an exhaustive search of the synchronization parameters. We then show that a relaxation of the aggregate SINR metric allows implementing an efficient multiuser analysis filter bank where the synchronization strategy consists in deploying a common time phase for all the users and in performing a partial correction of the frequency offsets. In this receiver, two fractionally spaced analysis stages are used. Each analysis stage is efficiently implemented via a polyphase DFT filter bank, followed by an extended DFT that allows the user frequency offsets to be partly compensated. This receiver has been already proposed in [12] with, however, a different synchronization metric and without the use of maximum SINR subchannel equalization. Furthermore, in this paper we discuss the application not only to multiuser FMT (as it was done in [12]) but also to OFDMA.

This paper is organized as follows. In Section 2, we describe the system model and the equalization scheme. In Section 3, we discuss synchronization based on maximum SINR, the efficient receiver analysis filter bank, and the application to FMT and OFDMA. A detailed derivation of the maximum SINR (MSINR) subchannel equalizer is reported in the appendix where we also discuss the relation with the minimum-mean-square-error (MMSE) equalization solution. The performance results are reported in Section 4. They show that, for the considered simulation scenario, multiuser

FMT performs better than OFDMA because of its better subchannel spectral containment. Finally, in Section 5 we draw the conclusions.

2. System Model

In a multiuser FBM system, the complex baseband signal $x^{(u)}(nT)$ transmitted by user u is obtained by a filter bank (FB) modulator with prototype pulse $g(nT)$, for example, a root-raised cosine pulse for FMT, and sub-carrier frequency $f_k = k/(MT)$, $k = 0, \dots, M-1$; that is,

$$\begin{aligned} x^{(u)}(nT) &= \sum_{k \in K_u} \sum_{\ell \in \mathbb{Z}} a^{(u,k)}(\ell T_0) g(nT - \ell T_0) e^{j2\pi f_k nT} \\ &= \sum_{k \in K_u} x^{(u,k)}(nT), \end{aligned} \quad (1)$$

where T is the sampling period, $K_u \subseteq \{0, \dots, M-1\}$ is the set of tone indices assigned to user u , and \mathbb{Z} is the set of integer numbers. $\{a^{(u,k)}(\ell T_0), \ell \in \mathbb{Z}\}$ is the k th subchannel data stream of user u that we assume to belong to the QPSK signal set, and that has period $T_0 = NT \geq MT$. With N_U users, $P = M/N_U$ subchannels are assigned to each user. The low-pass received signal is

$$\begin{aligned} y(iT) &= \sum_{u=0}^{N_U-1} \sum_{k \in K_u} \sum_{n \in \mathbb{Z}} x^{(u,k)}(nT) g_{\text{CH}}^{(u)}(iT - nT - \Delta_\tau^{(k)}) \\ &\quad \times e^{j2\pi \Delta_f^{(k)} iT} + \eta(iT), \end{aligned} \quad (2)$$

where $\Delta_\tau^{(k)}$ and $\Delta_f^{(k)}$ are the time and frequency offsets of the subchannel k assigned to user u . $g_{\text{CH}}^{(u)}(iT)$ is the fading channel impulse response of user u , and $\eta(iT)$ is the zero mean additive white complex Gaussian noise contribution. The time/frequency offsets are identical for all the subchannels of a given user, that is, $\Delta_\tau^{(k)} = \Delta_{\tau,u}$ and $\Delta_f^{(k)} = \Delta_{f,u}$, for $k \in K_u$.

Assuming to deploy a single-user receiver approach, the receiver (Figure 1) first compensates the frequency offset for the subchannels of the desired user by an amount $\tilde{\Delta}_f^{(k)}$; that is, the received signal $y(iT)$ is premultiplied by $e^{-j2\pi \tilde{\Delta}_f^{(k)} iT}$. Then, it applies an analysis filter and it uses a subchannel time phase $\tilde{\Delta}_\tau^{(k)}$ to correct the subchannel time offset. Its output for the k th subchannel can be written as

$$\begin{aligned} z^{(k)}(mT_0 + \tilde{\Delta}_\tau^{(k)}) &= \sum_{i \in \mathbb{Z}} y(iT) h(mT_0 - iT + \tilde{\Delta}_\tau^{(k)}) e^{-j2\pi(f_k + \tilde{\Delta}_f^{(k)}) iT} \\ &= e^{j(2\pi \beta_f^{(k)} mT_0 + \varphi^{(k)})} a^{(u,k)}(mT_0) g_{\text{EQ}}^{(k)}(0) \\ &\quad + e^{j(2\pi \beta_f^{(k)} mT_0 + \varphi^{(k)})} \sum_{m \neq \ell} a^{(u,k)}(\ell T_0) g_{\text{EQ}}^{(k)}(mT_0 - \ell T_0) \\ &\quad + \text{ICI}^{(k)}(mT_0 + \tilde{\Delta}_\tau^{(k)}) + \text{MAI}^{(k)}(mT_0 + \tilde{\Delta}_\tau^{(k)}) \\ &\quad + \eta^{(k)}(mT_0 + \tilde{\Delta}_\tau^{(k)}), \end{aligned} \quad (3)$$

where $\beta_f^{(k)} = \Delta_f^{(k)} - \tilde{\Delta}_f^{(k)}$ and $\varphi^{(k)} = 2\pi(\beta_f^{(k)} \tilde{\Delta}_\tau^{(k)} - f_k \Delta_\tau^{(k)})$. In (3) we have a term associated to the data symbol of interest, plus ISI, ICI, MAI, and noise. Further, the equivalent response of subchannel k of user u (that gives the ISI coefficients) reads

$$\begin{aligned} g_{\text{EQ}}^{(k)}(mT_0) &= \sum_{i \in \mathbb{Z}} g_{\text{CH}}^{(u)}(iT) e^{-j2\pi f_k iT} \\ &\quad \times \sum_{n \in \mathbb{Z}} g(nT - iT + mT_0 - \Delta_\tau^{(k)} + \tilde{\Delta}_\tau^{(k)}) \\ &\quad \times h(-nT) e^{j2\pi \beta_f^{(k)} nT}, \end{aligned} \quad (4)$$

where $k \in K_u$.

The filter bank outputs at rate $1/T_0$ are firstly compensated to remove the phase rotation introduced by the residual carrier frequency offset $\beta_f^{(k)}$, and then, they are processed with subchannel equalizers that we design according to the maximum SINR (MSINR) criterion. That is, we determine the N_w -length equalizer coefficients $\mathbf{w}_{\text{SINR}}^{(k)} = [w_0^{(k)} w_1^{(k)} \dots w_{N_w-1}^{(k)}]^T$ (where $(\cdot)^T$ denotes the transpose operator), that maximize the output SINR (see appendix)

$$\text{SINR}^{(k)}(\tilde{\Delta}_\tau^{(k)}, \tilde{\Delta}_f^{(k)}) = \frac{P_U^{(k)}(\tilde{\Delta}_\tau^{(k)}, \tilde{\Delta}_f^{(k)})}{P_I^{(k)}(\tilde{\Delta}_\tau^{(k)}, \tilde{\Delta}_f^{(k)}) + P_\eta^{(k)}(\tilde{\Delta}_\tau^{(k)}, \tilde{\Delta}_f^{(k)})}, \quad (5)$$

where $P_U^{(k)}$, $P_I^{(k)}$, and $P_\eta^{(k)}$ are the useful term average power, the interference and the noise power, at the equalizer output, respectively. These quantities, and thus the SINR at the equalizer output, depend on the synchronization parameters $\tilde{\Delta}_\tau^{(k)}$, and $\tilde{\Delta}_f^{(k)}$.

The SINR criterion, for given values of $\tilde{\Delta}_\tau^{(k)}$ and $\tilde{\Delta}_f^{(k)}$, yields the following solution for the equalizer coefficients

$$\mathbf{w}_{\text{SINR}}^{(k)} = (\mathbf{R}_{\text{SINR}}^{(k)})^{-1} \mathbf{p}_d^{(k)}, \quad (6)$$

where $\mathbf{R}_{\text{SINR}}^{(k)} = \mathbf{R}_{\text{ISI}}^{(k)} + \mathbf{R}_{\text{ICI+MAI}}^{(k)} + \mathbf{R}_\eta^{(k)}$ is the $N_w \times N_w$ correlation matrix of the interference-plus-noise term that comprises ISI, ICI, MAI, and noise, while $\mathbf{p}_d^{(k)} = [g_{\text{EQ}}^{(k)}(dT_0), \dots, g_{\text{EQ}}^{(k)}((N_w + d - 1)T_0)]^T$ is the subchannel response vector whose components are given by the equivalent impulse response coefficients in (4). The latter is a function of the total delay d of the system. The detailed derivation of the MSINR equalizer is reported in appendix. In the appendix we also report a proof that the maximum SINR solution is equivalent to the minimum-mean-square error (MMSE) equalizer solution [13] if, however, the ICI and MAI are taken into account in the computation of the equalizer coefficients.

For given values of $\tilde{\Delta}_\tau^{(k)}$ and $\tilde{\Delta}_f^{(k)}$, the MSINR equalizer yields the following output SINR (see appendix):

$$\text{SINR}_{\text{MAX}}^{(k)}(\tilde{\Delta}_\tau^{(k)}, \tilde{\Delta}_f^{(k)}) = (\mathbf{p}_d^{(k)})^H (\mathbf{R}_{\text{SINR}}^{(k)})^{-1} \mathbf{p}_d^{(k)}, \quad (7)$$

where $(\cdot)^H$ denotes the Hermitian operator, and for ease of notation, we do not explicitly show the dependency of the

correlation matrix and of the subchannel response vector from $\tilde{\Delta}_\tau^{(k)}$ and $\tilde{\Delta}_f^{(k)}$.

Now, in OFDM [2] the synthesis pulse is $g(nT) = \text{rect}(nT/T_0)$ while the analysis pulse is $h(nT) = \text{rect}(-(n + \mu)T/MT)$, where the rectangular pulse is defined as $\text{rect}(t) = 1$ for $0 \leq t < 1$, and zero otherwise. $\mu = N - M$ is the cyclic prefix (CP) length in samples. The efficient implementation of OFDM is done with an inverse DFT (IDFT) plus the insertion of the CP at the transmitter. At the receiver, after synchronization, the CP is discarded and a DFT is applied. Commonly, one-tap subchannel equalization is used. In the multiuser channel, orthogonality can be preserved for the subchannels of the desired user. However, MAI is introduced when the other users' have distinct carrier frequency offsets, and propagation delays plus channel dispersion in excess of the CP length [7].

In FMT [3], the subchannel symbol period is $T_0 = NT$. The analysis pulse is matched to the synthesis pulse, that is, $h(nT) = g^*(-nT)$. The peculiarity is that the subchannels are shaped with time-frequency concentrated pulses, for example, root-raised-cosine pulses. This allows minimizing the ICI and therefore the MAI. Linear subchannel equalization, as described above, is used to cope with the residual subchannel ISI. The analysis FB can be efficiently implemented via polyphase filtering followed by an M -point DFT [3, 4] provided that the subchannel analysis pulses are identical and the time/frequency compensation is identical for all the subchannels.

3. Maximum SINR Synchronization Metrics

The choice of the synchronization parameters affects not only the performance but also the implementation complexity of the receiver as discussed in the following.

The most intuitive thing we can do is to compensate the time and frequency offset for each user with the exact value of the misalignments; that is, $\tilde{\Delta}_\tau^{(k)} = \Delta_{\tau,u}$ and $\tilde{\Delta}_f^{(k)} = \Delta_{f,u}$ for $k \in K_u$. As shown in Section 4, this baseline receiver (BL-RX) may yield suboptimal performance. Therefore, the criterion herein considered is to choose $\tilde{\Delta}_\tau^{(k)}$ and $\tilde{\Delta}_f^{(k)}$ such that the SINR in (5) or an average SINR is maximized.

The best approach is to perform synchronization at subchannel level, that is, we use for each subchannel an optimal value for the parameters. This is because in the presence of frequency selective fading the channel responses vary across the subchannels. Further, each subchannel experiences a different amount of MAI which depends on the realization of the time/frequency offsets of the other subchannels assigned to the users. Therefore, for each subchannel k belonging to user u , we have to find the frequency offset $\tilde{\Delta}_f^{(k)}$ and the sampling phase $\tilde{\Delta}_\tau^{(k)}$ that maximize the SINR (5) at the output of the subchannel equalizer; that is,

$$\left(\tilde{\Delta}_\tau^{(k)}, \tilde{\Delta}_f^{(k)}\right) = \arg \max_{\substack{-1/(2MT) < \Delta_f < 1/(2MT) \\ -NT \leq \Delta_\tau \leq NT}} \left[\text{SINR}^{(k)}(\Delta_\tau, \Delta_f) \right]. \quad (8)$$

In (8) we assume $|\tilde{\Delta}_f^{(k)}| < 1/(2MT)$, so that adjacent subchannels do not completely overlap. Moreover, we assume

that we have performed a coarse time synchronization, so we can bound the sampling phase search in the interval $[-NT, NT]$, corresponding to twice the symbol period.

It should be noted that there are two sources of complexity. First, the exhaustive search of the optimal parameters according to (8) is a heavy task. It implies the direct computation of the maximum SINR at the subchannel equalizer output according to (7) for each possible value of $\tilde{\Delta}_\tau^{(k)}$ and $\tilde{\Delta}_f^{(k)}$. Second, we cannot process all the subchannels with an efficient polyphase DFT analysis FB since this requires a common time/frequency compensation for all the subchannels [3, 4]. If we assume the prototype pulse to have length LN coefficients, the complexity of the receiver filter bank is in the order of $2MLN^2/T_0$ complex operations (addition and multiplications) per second.

To lower the complexity, we have to use a common sampling phase and a common frequency offset compensation for all the subchannels assigned to the user. This receiver is referred to as User Synchronized Receiver (US-RX) and it deploys the parameters obtained by maximizing the average user SINR as follows:

$$\left(\tilde{\Delta}_\tau^{(u)}, \tilde{\Delta}_f^{(u)}\right) = \arg \max_{\substack{-1/(2MT) < \Delta_f < 1/(2MT) \\ -NT \leq \Delta_\tau \leq NT}} \left[\sum_{k \in K_u} \text{SINR}^{(k)}(\Delta_\tau, \Delta_f) \right]. \quad (9)$$

We note that according to (9) we do not necessarily completely compensate the time and frequency offset of the user of interest. This is the case only in the absence of MAI because in such a case the SINR equals the SNR which is maximized with an analysis FB perfectly matched to the synthesis FB. It should be noted that also this synchronization strategy requires an exhaustive joint search of the optimal synchronization parameters $(\tilde{\Delta}_\tau^{(u)}, \tilde{\Delta}_f^{(u)})$ and the computation of the SINR has to be done at sampling rate $1/T$. In other words, during the synchronization stage we cannot implement the analysis filter bank in an efficient manner. On the contrary, during the detection stage the received signal is time/frequency precompensated with the use of the estimated parameters $(\tilde{\Delta}_\tau^{(u)}, \tilde{\Delta}_f^{(u)})$ and analyzed with a filter bank that can be efficiently implemented via polyphase filtering and a DFT [3, 4]. However, we still need to run one analysis FB per user. The DFT filter bank is discussed in Section 3.1 and 3.2.

It would be beneficial to use a unique analysis FB that allowed the detection of all users' signals. To do so we have to find a common sampling phase $\tilde{\Delta}_\tau$ and a common frequency offset compensation by $\tilde{\Delta}_f$ for all the users. This can be done by maximizing the aggregate SINR as follows:

$$\left(\tilde{\Delta}_\tau, \tilde{\Delta}_f\right) = \arg \max_{\substack{-1/(2MT) < \Delta_f < 1/(2MT) \\ -NT < \Delta_\tau < NT}} \left[\sum_{k=0}^{M-1} \text{SINR}^{(k)}(\Delta_\tau, \Delta_f) \right]. \quad (10)$$

In the following, this receiver is referred to as Multiuser Analysis FB (MU-FB).

3.1. Efficient Implementation of the Multiuser Analysis Filter Bank. As explained in the previous section, the most efficient solution (in terms of implementation complexity) is the MU-FB, where all the users' signals are detected by a single analysis bank using the same sampling phase $\tilde{\Delta}_\tau$ and the same frequency offset compensation by $\tilde{\Delta}_f$ for all the subchannels. An efficient implementation of this receiver is possible, and it has been proposed in [12]. For clarity we summarize the main steps and we further extend the results. It is obtained via the polyphase decomposition of the received signal (after time and frequency compensation) with period $T_2 = M_2 T$, where $M_2 = \ell.c.m.(M, N) = K_2 M = L_2 N$, and $\ell.c.m.(M, N)$ is the least common multiple between M and N . The polyphase decomposition of the received signal can be written as

$$y^{(i)}(\ell L_2 T_0) = y(iT + \ell L_2 T_0 + \tilde{\Delta}_\tau) e^{-j2\pi\tilde{\Delta}_f(iT + \ell L_2 T_0)}, \quad (11)$$

$$i = 0, \dots, M_2 - 1.$$

Since $f_k = k/MT = K_2 k/M_2 T$, the k th subchannel output is computed as follows:

$$z^{(k)}(mT_0) = \sum_{i=0}^{M_2-1} Z^{(i)}(mT_0) e^{-j(2\pi K_2/M_2)ik}, \quad (12)$$

$$k = 0, \dots, M - 1,$$

$$Z^{(i)}(mT_0) = \sum_{\ell \in \mathbb{Z}} y^{(i)}(\ell L_2 T_0) h^{(-i)}(mT_0 - \ell L_2 T_0),$$

where $h^{(-i)}(mT_0) = h(mT_0 - iT)$ is the i th polyphase pulse component. According to (12) the efficient realization comprises the following steps: compensate the time/frequency offset, serial-to-parallel (S/P) convert the signal, interpolate the M_2 polyphase components of the compensated signal by a factor L_2 , analyze them with the low-rate filters $h^{(-i)}(mT_0)$, apply an M_2 -point DFT, and sample the outputs of index $K_2 k$. The indices $k \in K_u$ are those associated to the subchannels of user u .

We note that we can relax the constraint of having an identical frequency offset compensation for all the subchannels by simply exploiting the frequency resolution provided by the DFT. To do this, we first define $M_3 = QM_2 = K_3 M = L_3 N$, where Q is a positive integer. Then, we split the subchannel frequency offset in an integer part, multiple of $1/M_3 T$, and a fractional part $\hat{\Delta}_f^{(k)}$; that is,

$$\Delta_f^{(k)} = \frac{q^{(k)}}{M_3 T} + \hat{\Delta}_f^{(k)}. \quad (13)$$

In the following we assume $|q^{(k)}| < \lfloor K_3/2 \rfloor$, so that adjacent subchannels do not completely overlap. Furthermore, we assume to compensate, before the FB, only the integer part of the frequency offset, and to sample the subchannel filter

output at time instant $mT_0 + \tilde{\Delta}_\tau$. Therefore, the subchannel output of index k is

$$z^{(k,q^{(k)})}(mT_0 + \tilde{\Delta}_\tau) = \sum_{i \in \mathbb{Z}} y(iT) e^{-j2\pi(f_k + (q^{(k)}/M_3 T))iT}$$

$$\times h(mT_0 + \tilde{\Delta}_\tau - iT)$$

$$= e^{j(2\pi\tilde{\Delta}_f^{(k)} mT_0 + \varphi^{(k)})} a^{(u,k)}(mT_0) g_{\text{EQ}}^{(k)}(0)$$

$$+ I^{(k)}(mT_0 + \tilde{\Delta}_\tau), \quad (14)$$

where $\varphi^{(k)} = 2\pi(\hat{\Delta}_f^{(k)} \tilde{\Delta}_\tau - f_k \Delta_\tau^{(k)})$. It comprises a useful term plus an interference term due to ISI, ICI, MAI, and noise. Furthermore, the subchannel equivalent response of subchannel $k \in K_u$ of user u reads

$$g_{\text{EQ}}^{(k)}(mT_0) = \sum_{i \in \mathbb{Z}} g_{\text{CH}}^{(u)}(iT) e^{-j2\pi f_k iT}$$

$$\times \sum_{n \in \mathbb{Z}} g(nT - iT + mT_0 - \Delta_\tau^{(k)} + \tilde{\Delta}_\tau) \quad (15)$$

$$\times h(-nT) e^{j2\pi\hat{\Delta}_f^{(k)} nT}.$$

The factor $e^{j2\pi\hat{\Delta}_f^{(k)} mT_0}$ in (14) introduces a time-variant rotation of the constellation, but it can be fully compensated at the subchannel filter output before passing the samples to the equalizer. The factor $e^{j2\pi\hat{\Delta}_f^{(k)} nT}$ in (15) cannot be compensated, and it yields a frequency mismatch between the received subchannel and the analysis subchannel filter. Therefore, the compensation of only the integer part of the frequency offset translates in both a subchannel SNR loss, and increased ISI. However, as it is shown in Section 4, the penalty in performance can be negligible for practical values of frequency offset, that is, when $\hat{\Delta}_f^{(k)} nT$ is small over the duration of the prototype pulse.

The correction of the integer part of the frequency offset can be included in the efficient implementation. If we apply the polyphase decomposition to (14) with period $M_3 T$, we obtain

$$z^{(k,q^{(k)})}(mT_0 + \tilde{\Delta}_\tau) = \sum_{i=0}^{M_3-1} Y^{(i)}(mT_0 + \tilde{\Delta}_\tau) \quad (16)$$

$$\times e^{-j(2\pi(K_3 k + q^{(k)})/M_3)i},$$

with

$$Y^{(i)}(mT_0 + \tilde{\Delta}_\tau) = \sum_{\ell \in \mathbb{Z}} y^{(i)}(\ell L_3 T_0 + \tilde{\Delta}_\tau)$$

$$\times h^{(-i)}(mT_0 - \ell L_3 T_0) \quad (17)$$

$$y^{(i)}(\ell L_3 T_0 + \tilde{\Delta}_\tau) = y(iT + \ell L_3 T_0 + \tilde{\Delta}_\tau),$$

$$i = 0, \dots, M_3 - 1.$$

According to (16) and (17), the efficient realization comprises the following steps (see also Figure 2): S/P conversion,

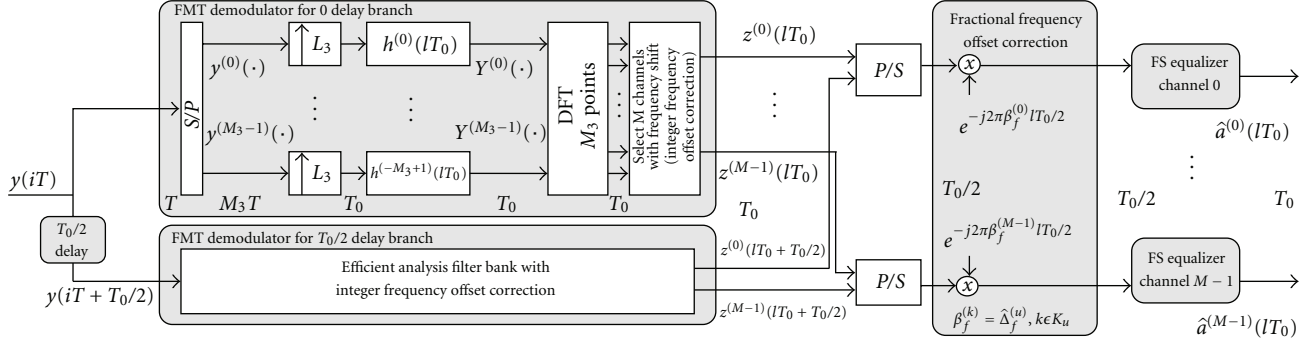


FIGURE 2: Multiuser analysis filter bank receiver.

interpolation by a factor L_3 , filtering with the polyphase pulses $h^{(-i)}(mT_0)$, computation of an M_3 -point DFT, and sampling the DFT outputs with index $K_3k + q^{(k)}$ for $k \in K_u$. Finally, we compensate the fractional frequency offset with the multiplication by $e^{-j2\pi\tilde{\Delta}_f^{(k)}mT_0}$ at the DFT stage output; that is, we remove the time variant phase shift of the signal at the subchannel equalizer input. Note that the correction of the integer part of the frequency offset is done by choosing the appropriate output tone of the M_3 -point DFT (shifted tone). With perfect compensation of the fractional frequency offset, the subchannel equalizer does not see any residual frequency offset; therefore, it is implemented with a static filter over a given burst of data symbols. In the presence of channel time variations, adaptation can also be performed at a symbol-by-symbol level.

With this efficient implementation, we have devised a unique FB that allows the choice of different frequency offsets (multiple of the DFT frequency resolution $1/M_3T$) for the different subchannels. Therefore, the synchronization metric (10) can be generalized as follows:

$$(\tilde{\Delta}_\tau, \tilde{\mathbf{q}}) = \arg \max_{\substack{-\lfloor K_3/2 \rfloor \leq q < \lfloor K_3/2 \rfloor \\ -NT < \tilde{\Delta}_\tau < NT}} \left[\sum_{k=0}^{M-1} \text{SINR}^{(k)}(\tilde{\Delta}_\tau, q^{(k)}) \right], \quad (18)$$

where $\mathbf{q} = [q^{(0)}, \dots, q^{(M-1)}]$ is the vector with components satisfying $|q^{(k)}| \leq \lfloor K_3/2 \rfloor$ for all $k \in \{0, \dots, M-1\}$. The metric (18) corresponds to find the sampling phase $\tilde{\Delta}_\tau$ and the set of integer parameters $\tilde{\mathbf{q}} = [\tilde{q}^{(0)}, \dots, \tilde{q}^{(M-1)}]$ that maximize the aggregate SINR. Moreover, differently from (8), (9), and (10) that require the maximization over an infinite set of frequency offsets, the search in (18) can be done over a discrete and finite set of q values.

In the next section, we specialize the MU-FB to two schemes of practical interest, that is, FMT and OFDM. We propose a further simplification for FMT that allows using a fractionally spaced analysis filter bank during both the synchronization stage and the detection stage.

3.2. Application of the MU-FB to FMT Systems. Since in FMT the subchannels are frequency confined, a wrong time phase may introduce increased subchannel ISI but it does not,

ideally, introduce ICI. Therefore, instead of searching the time phase according to (18) (which has to be done at least with resolution equal to the sampling period T), we propose to deploy two multiuser analysis FBs, the first with a fixed sampling phase $\tilde{\Delta}_\tau = 0$, and the second with $\tilde{\Delta}_\tau = T_0/2$. The outputs of the two FBs are processed by fractionally spaced linear subchannel equalizers [13], as shown in Figure 2. They are designed according to the MSINR criterion (see appendix). In this case, (18) reduces to the independent search of the parameters $\tilde{q}^{(k)}$ as follows:

$$\tilde{q}^{(k)} = \arg \max_{-\lfloor K_3/2 \rfloor \leq q < \lfloor K_3/2 \rfloor} \left[\text{SINR}_F^{(k)}(q) \right], \quad (19)$$

where $\text{SINR}_F^{(k)}(q)$ is the output SINR of the fractionally spaced equalizer applied to subchannel k assuming a frequency offset compensation equal to q/M_3T .

Extending the result in (6) and (7) (see appendix), the MSINR fractionally spaced equalizer solution is given by

$$\mathbf{w}_{F, \text{SINR}}^{(k)} = \left(\mathbf{R}_{F, \text{SINR}}^{(k)} \right)^{-1} \mathbf{p}_{F,d}^{(k)}, \quad (20)$$

while

$$\text{SINR}_F^{(k)}(q) = \left(\mathbf{p}_{F,d}^{(k)} \right)^H \left(\mathbf{R}_{F, \text{SINR}}^{(k)} \right)^{-1} \mathbf{p}_{F,d}^{(k)}, \quad (21)$$

where $\mathbf{R}_{F, \text{SINR}}^{(k)}$ is the $2N_w \times 2N_w$ correlation matrix of the interference-plus-noise term that comprises ISI, ICI, and MAI, while $\mathbf{p}_{F,d}^{(k)}$ is the subchannel response vector whose components are given by the equivalent impulse response coefficients (15) sampled, however, at rate $2/T_0$, that is, $\mathbf{p}_{F,d}^{(k)} = [g_{\text{EQ}}^{(k)}(dT_0/2), \dots, g_{\text{EQ}}^{(k)}((2N_w + d - 1)T_0/2)]^T$.

If the amount of the interference is small, the optimal $\tilde{q}^{(k)}$ value is obtained as follows:

$$\tilde{q}^{(k)} = \arg \min_{-\lfloor K_3/2 \rfloor \leq q < \lfloor K_3/2 \rfloor} \left[\left| \Delta_f^{(k)} - \frac{q}{M_3T} \right| \right], \quad (22)$$

that corresponds to minimize the fractional part of the frequency offset at the output of the receiver FB; that is, we compensate almost perfectly the frequency offset. This metric that was used in [12], is simpler than (19), but

it provides, in general, lower performance as shown in Section 4.

It should be noted that now both the synchronization stage and the detection stage enjoy the same efficient implementation of the fractionally spaced analysis filter bank whose complexity is in the order of $2(2LN + QM_2 \log_2(QM_2) - QM_2)/T_0$ operations per second. On the contrary, the US-RX enjoys the efficient implementation only during the detection stage which is equal to $N_U(2LN + M_2 \log_2(M_2) - M_2)/T_0$ operations per second for the overall N_U users. Therefore, also during the detection stage the US-RX can be more complex than the fractionally spaced MU-RX depending on the choice of the parameters. For instance, with $M = 32$, $N = 40$, $L = 6$, and $N_U = 8$, the filter bank in the SU-RX during synchronization has complexity 15360 operation/s while it has complexity 298 operation/s during detection. The MU-RX analysis filter bank has complexity both during synchronization and detection equal to 74, 290, 620 operations/s, respectively, for $Q = 1, 4, 8$.

3.3. Application of the MU-FB to OFDM Systems. As it is known, the OFDM systems are extremely sensitive to time and frequency misalignments [6–8]. This is due to the fact that the prototype pulse has a *sinc* frequency response. Thus, differently from FMT, it does not provide a high frequency confinement. To provide robustness we may synchronize the users in the downlink frame and deploy a CP that is longer than the channel time dispersion plus the maximum delay of the users [7]. Under this assumption, we can use a common $\tilde{\Delta}_\tau$ for all the users that is equal to the sampling phase that synchronizes the receiver to the user with the minimum delay. Thus, differently from the FMT case, we can use a single multiuser analysis FB, and the choice of the set of parameters $\tilde{\mathbf{q}}$ can be independently performed from $\tilde{\Delta}_\tau$ according to (19).

It should be noted that, in the OFDM case, the implementation of the multiuser analysis FB herein proposed, comprises the following steps. First, we acquire synchronization with the user having minimum delay and we discard the CP. Then, we zero pad the frame of M received samples to obtain a frame of M_3 samples, and we apply an M_3 -point DFT.

Finally, we point out that to mitigate the MAI interference in OFDMA, some multiuser detection approach may be necessary, for example, maximum likelihood [1] detection or linear multichannel [14] equalization. This, however, increases complexity.

4. Performance Results

We now compare the performance of the various synchronization metrics. We first consider 8 asynchronous users, $M = 32$ tones that are regularly interleaved across the users both in the FMT and the OFDM systems. To obtain the same transmission rate, we use an interpolation factor of $N = 40$ in FMT, and a CP = 8 samples in OFDM. In the FMT system, the prototype pulse has duration $12T_0$, and it is designed according to [4] to achieve a theoretical

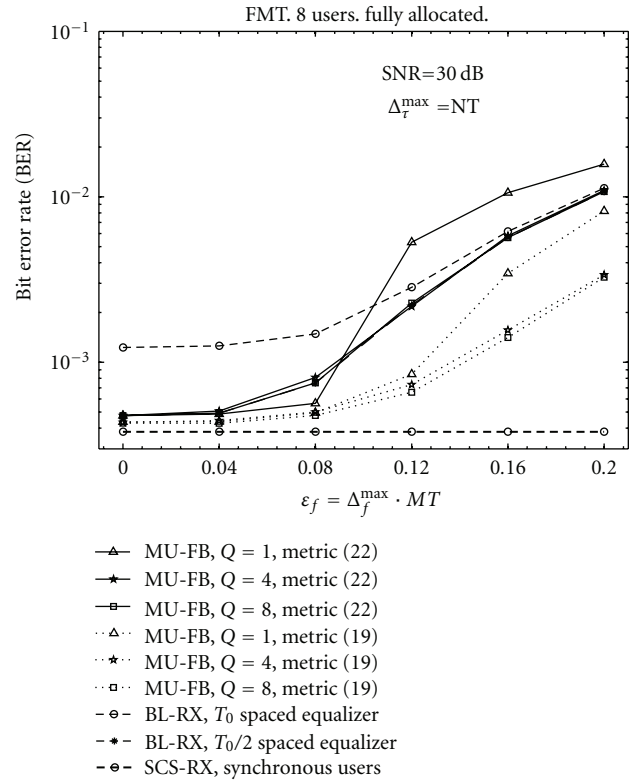


FIGURE 3: BER as a function of frequency offset. 8 interleaved users fully allocated. Comparison of the compensation metrics for different values of Q . FMT with $M = 32$ and $N = 40$.

bandwidth equal to $1.25/T_0 = 1/MT$. We assume the carrier frequency offsets to be independent and uniformly distributed in $[-\Delta_f^{\max}, \Delta_f^{\max}]$, while the time offsets to be uniformly distributed in $[0, \Delta_\tau^{\max}]$, with $\Delta_\tau^{\max} = NT$. The user channels are assumed to be Rayleigh faded with an exponential power delay profile with independent T -spaced taps that have average power $\Omega_p \sim e^{-pT/(0.05T_0)}$ with $p \in \mathbb{Z}^+$ and truncation at -20 dB. Perfect knowledge of the parameters (time/frequency offsets) and channel responses is assumed. QPSK modulation is used. OFDM performs one-tap equalization, while FMT deploys three taps subchannel equalization. The average bit error rate (BER) is obtained by averaging the BER of all the users over bursts of duration 100 symbols.

In Figures 3–6 we plot the BER as function of the maximum carrier frequency offset. The SNR is set to 30 dB. The SNR includes the loss in OFDM due to the cyclic prefix. We compare the performance obtained with the base line receiver (BL-RX) to the performance of the MU-FB receiver that uses the metric (19), labelled with “metric (19)”, or the metric (22), labelled with “metric (22)”. For the FMT case the BL-RX uses a T_0 spaced equalizer or a $T_0/2$ fractionally spaced equalizer. The BL-RX is a single-user receiver that performs perfect compensation of the time/frequency offset for the user of interest. As discussed in Section 3, the BL-RX is identical to the US-RX in the absence of MAI. Therefore, for small carrier frequency offsets the performance of the two

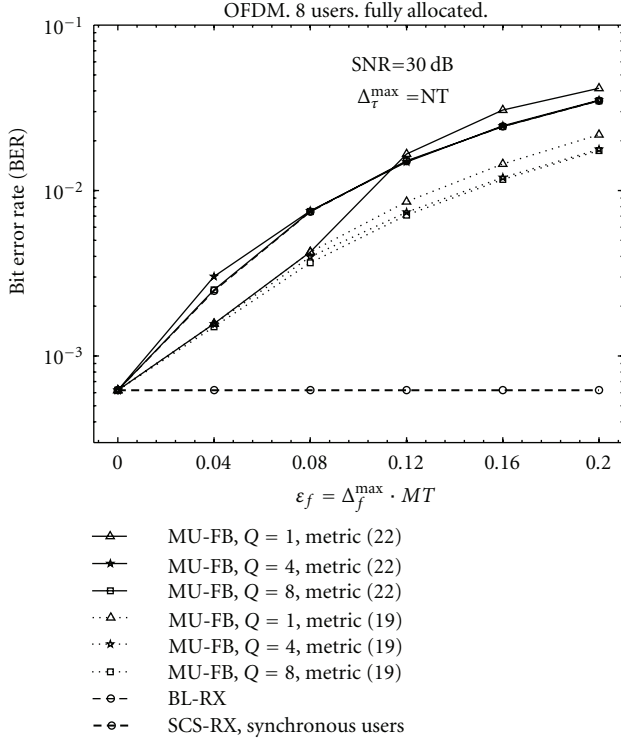


FIGURE 4: BER as a function of frequency offset. 8 interleaved users fully allocated. Comparison of the compensation metrics for different values of Q . OFDM with $M = 32$ and $CP = 8$.

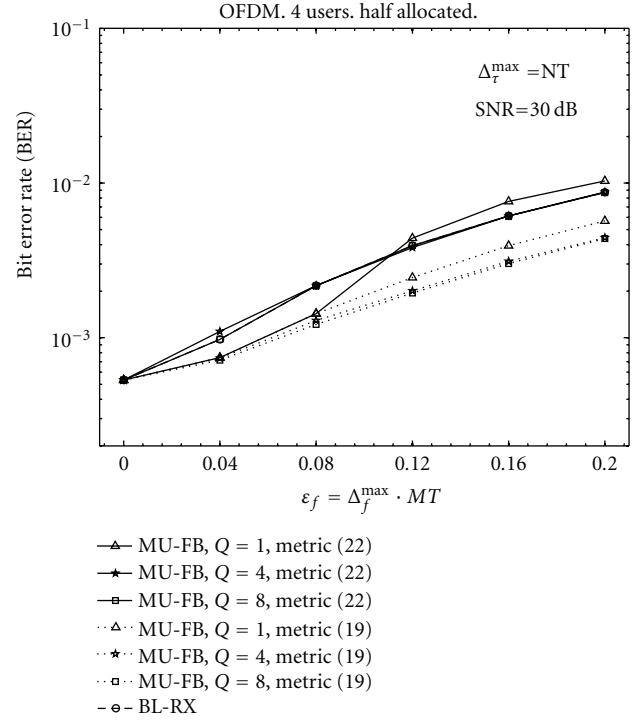


FIGURE 6: BER as a function of frequency offset. 8 interleaved users with only 4 nonadjacent active users. Comparison of the compensation metrics for different values of Q . OFDM with $M = 32$ and $CP = 8$.

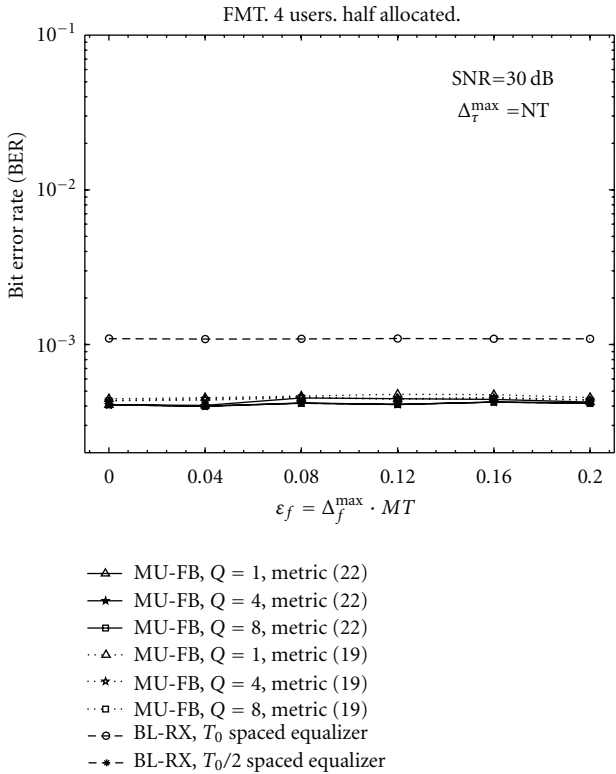


FIGURE 5: BER as a function of frequency offset. 8 interleaved users with only 4 nonadjacent active users. Comparison of the compensation metrics for different values of Q . FMT with $M = 32$ and $N = 40$.

receivers in the FMT system, is similar since the subchannels exhibit a good frequency confinement.

The curve labelled with “SCS-RX, synchronous users” shows the performance with synchronous users and with the use of metric (8). It essentially shows the best attainable performance.

The MU-FB with the metric that maximizes the SINR (metric (19)) performs well for all the range of frequency offsets both for FMT and OFDM. Especially for high values of $\epsilon_f = \Delta_f^{\max} MT$ it performs better than with the metric that minimizes the residual frequency offset (metric (22)) which does not take into account the presence of MAI. Further, the performance of the MU-FB with metric (19) improves as Q increases. This is because a higher frequency resolution is provided and therefore improved compensation capability of the carrier frequency offsets is obtained. FMT provides significant better BER performance than OFDM due to its better subchannel spectral containment that reduces the effect of the MAI.

In Figures 5–6 we consider the same scenario of Figures 3–4 but only 4 nonadjacent users, with 4 tones each, are active (users number 1, 3, 5, 7). In this case the MAI is significantly reduced because each tone has two null adjacent tones. FMT is essentially not affected by the carrier frequency offsets, while OFDM still exhibits a high BER penalty. The MU-FB and the BL-RX with a $T_0/2$ fractionally spaced equalizer in FMT have similar performance while in OFDM the MU-FB provides performance gains.

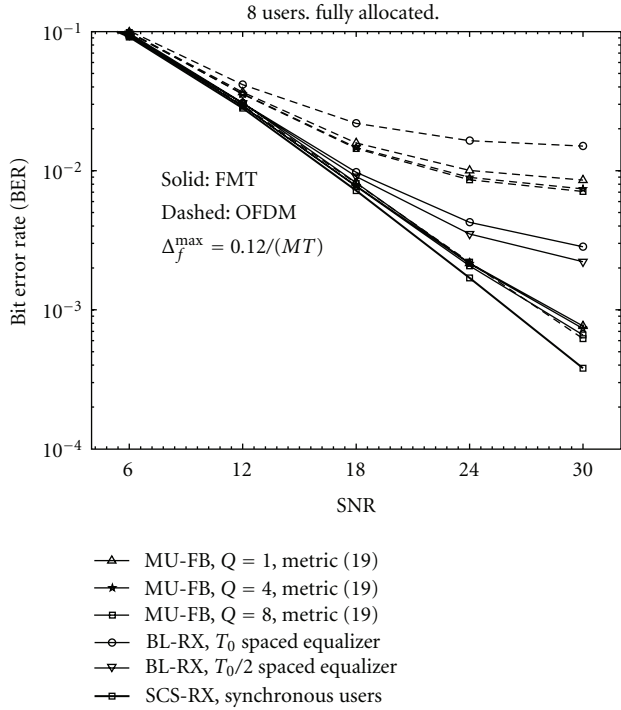


FIGURE 7: BER as a function of SNR. 8 interleaved users fully allocated. FMT with $M = 32$ and $N = 40$. OFDM with $M = 32$ and $CP = 8$.

In Figure 7 we plot the average BER as a function of the SNR. We consider 8 users fully allocated and a maximum frequency offset $\Delta_f^{\max} = 0.12/(MT)$. We show, both for FMT and OFDM, the performance of metric (19) for different values of Q . FMT has always better performance and it exhibits lower error floors for high SNRs. We also report the BER with synchronous users (curve labelled with “SCS-RX, synchronous users”). In this case FMT has better performance than OFDM because the subchannel equalizer is capable of exploiting some frequency diversity.

5. Conclusions

In this paper we have discussed maximum SINR synchronization in multiuser FBM systems. Perfect-user synchronization is not necessarily optimal with single user detection. The optimal subchannel synchronized receiver aims at maximizing the SINR at subchannel level, but it is complex and cannot enjoy an efficient DFT-based realization. Per-user synchronization requires a bank of single-users receivers. A single analysis filter bank can be implemented if a common compensation of the users time/frequency offset is performed, for example, according to an aggregate SINR criterion.

We have then proposed a suboptimal SINR metric that allows the realization of a multiuser low complexity fractionally spaced analysis FB combined with subchannel MSINR fractionally spaced equalization. This receiver is in principle applicable to any FBM system. We have discussed its application to OFDMA and multiuser FMT. We have

highlighted that it performs better with the novel MSINR metric herein proposed than with the one used in [12] that targets perfect frequency offset compensation without taking into account the presence of interference. Furthermore, simulation results show that FMT exhibits superior performance than OFDMA since it has more robustness to the MAI due to the better subchannel spectral containment.

Finally, we have reported (see appendix) a proof that the maximum SINR subchannel equalizer is equal to the MMSE subchannel equalizer if we take into account the presence of interference.

Appendices

A. Linear Subchannel Equalizer Design

In this appendix we first report the derivation of the maximum SINR equalizer. Then, we prove that this solution is equivalent to the MMSE one; that is, the MMSE criterion for channel equalization design maximizes the SINR at the equalizer output provided that the presence of ICI and ISI is taken into account.

A.1. Maximum SINR Subchannel Equalizer. The signal at the equalizer output can be written as follows. ($E[\cdot]$ denotes the expectation operator.)

$$\hat{\mathbf{a}}_m^{(k)} = \hat{\mathbf{a}}^{(k)}(mT_0) = (\mathbf{w}^{(k)})^H \mathbf{z}_m^{(k)}, \quad (\text{A.1})$$

where $\mathbf{w}^{(k)} = [w_0^{(k)} w_1^{(k)} \dots w_{N_w-1}^{(k)}]^T$ is a column vector containing the N_w coefficients of the equalization filter, while $\mathbf{z}_m^{(k)} = [z_m^{(k)} z_{m-1}^{(k)} \dots z_{m-(N_w-1)}^{(k)}]^T$ is a column vector containing the samples at the subchannel equalizer input that are given by (3) after the compensation of the residual carrier frequency offset via multiplication by $e^{-j(2\pi\beta_f^{(k)} mT_0 + \varphi^{(k)})}$. The vector $\mathbf{z}_m^{(k)}$ can be written as follows:

$$\mathbf{z}_m^{(k)} = \sum_{\hat{k}=0}^{M-1} \mathbf{P}_m^{(\hat{k},k)} \mathbf{a}_m^{(\hat{k})} + \boldsymbol{\eta}_m^{(k)}, \quad (\text{A.2})$$

where $\mathbf{P}_m^{(\hat{k},k)} = [\mathbf{p}_{m,1}^{(\hat{k},k)} \mathbf{p}_{m,2}^{(\hat{k},k)} \dots \mathbf{p}_{m,N_p+N_w-1}^{(\hat{k},k)}]$ is a Toeplitz matrix of size $[N_w \times (N_p + N_w - 1)]$ containing the coefficients of the equivalent cross-channel impulse response, at time instant m , between the input subchannel of index \hat{k} and the output subchannel of index k in the system, which can be obtained with a generalization of (4) (see also the Appendix A in [12]) and which is assumed to have duration N_p coefficients. The column vector $\mathbf{a}_m^{(k)} = [a_{m+N_p/2-1}^{(k)} \dots a_{m-1}^{(k)} \dots a_{m-N_p/2-N_w+1}^{(k)}]^T$ contains the transmitted data symbols that are assumed to be independent, with zero mean, and with unitary power, that is, $E[\mathbf{a}_m^{(k)} (\mathbf{a}_m^{(k)})^H] = \mathbf{I}_{N_p+N_w-1}$, where $\mathbf{I}_{N_p+N_w-1}$ is an identity matrix of size $N_p + N_w - 1$. In general, the noise vector of samples has correlation $E[\boldsymbol{\eta}_m^{(k)} (\boldsymbol{\eta}_m^{(k)})^H] = \mathbf{R}_\eta^{(k)}$. Assuming the analysis prototype pulse to be a Nyquist pulse and the input noise to be white Gaussian, we have that $\mathbf{R}_\eta^{(k)} = N_0 \mathbf{I}_{N_w}$.

Substituting (A.2) in (A.1) and assuming a total delay of d samples in the system, we have

$$\begin{aligned}\hat{a}_m^{(k)} &= \sum_{n=0}^{N_w-1} w_n^* z_{m-n}^{(k)} = \left(\mathbf{w}^{(k)} \right)^H \left(\sum_{\hat{k}=0}^{M-1} \mathbf{P}_m^{(\hat{k},k)} \mathbf{a}_m^{(\hat{k})} + \boldsymbol{\eta}_m^{(k)} \right) \\ &= \underbrace{\left(\mathbf{w}^{(k)} \right)^H \mathbf{P}_d^{(k)} \mathbf{a}_{m-d}^{(k)}}_{\text{useful signal}} + \underbrace{\sum_{\ell \neq d} \left(\mathbf{w}^{(k)} \right)^H \mathbf{P}_\ell^{(k)} \mathbf{a}_{m-\ell}^{(k)}}_{\text{ISI}} \\ &\quad + \underbrace{\sum_{\hat{k} \neq k} \left(\mathbf{w}^{(k)} \right)^H \mathbf{P}_m^{(\hat{k},k)} \mathbf{a}_m^{(\hat{k})}}_{\text{ICI and MAI}} + \underbrace{\left(\mathbf{w}^{(k)} \right)^H \boldsymbol{\eta}_m^{(k)}}_{\text{noise}},\end{aligned}\quad (\text{A.3})$$

where $\mathbf{p}_d^{(k)} = [\mathbf{g}_{\text{EQ}}^{(k)}(dT_0), \dots, \mathbf{g}_{\text{EQ}}^{(k)}((N_w + d - 1)T_0)]^T$ has elements given by (4).

To derive the equalizer that maximizes the SINR, we start from the computation of the signal-to-interference-plus-noise ratio at the equalizer output. From (A.3), the useful signal power, for a given delay d , is

$$P_U^{(k)} = \left(\mathbf{w}_{\text{SINR}}^{(k)} \right)^H \mathbf{p}_d^{(k)} \left(\mathbf{p}_d^{(k)} \right)^H \mathbf{w}_{\text{SINR}}^{(k)}. \quad (\text{A.4})$$

The noise plus interference power is

$$\begin{aligned}P_I^{(k)} + P_\eta^{(k)} &= \underbrace{\sum_{\ell \neq d} \left(\mathbf{w}_{\text{SINR}}^{(k)} \right)^H \mathbf{P}_\ell^{(k)} \left(\mathbf{P}_\ell^{(k)} \right)^H \mathbf{w}_{\text{SINR}}^{(k)}}_{\text{ISI}} \\ &\quad + \underbrace{\sum_{\hat{k} \neq k} \left(\mathbf{w}_{\text{SINR}}^{(k)} \right)^H \mathbf{P}_m^{(\hat{k},k)} \left(\mathbf{P}_m^{(\hat{k},k)} \right)^H \mathbf{w}_{\text{SINR}}^{(k)}}_{\text{ICI and MAI}} \\ &\quad + \underbrace{\left(\mathbf{w}_{\text{SINR}}^{(k)} \right)^H \mathbf{R}_\eta^{(k)} \mathbf{w}_{\text{SINR}}^{(k)}}_{\text{noise}}.\end{aligned}\quad (\text{A.5})$$

Then, the SINR can be written as follows:

$$\begin{aligned}\text{SINR}^{(k)} &= \frac{(\mathfrak{D})^H \mathbf{R}_U^{(k)} \mathfrak{D}}{(\mathfrak{D})^H \mathbf{R}_{\text{ISI}}^{(k)} \mathfrak{D} + (\mathfrak{D})^H \mathbf{R}_{\text{ICI+MAI}}^{(k)} \mathfrak{D} + (\mathfrak{D})^H \mathbf{R}_\eta^{(k)} \mathfrak{D}},\end{aligned}\quad (\text{A.6})$$

where \mathfrak{D} denotes $\mathbf{w}_{\text{SINR}}^{(k)}$, $\mathbf{R}_U^{(k)} = \mathbf{p}_d^{(k)} \left(\mathbf{p}_d^{(k)} \right)^H$, $\mathbf{R}_{\text{ISI}}^{(k)} = \sum_{\ell \neq d} \mathbf{P}_\ell^{(k)} \left(\mathbf{P}_\ell^{(k)} \right)^H$, and $\mathbf{R}_{\text{ICI+MAI}}^{(k)} = \sum_{\hat{k} \neq k} \mathbf{P}_m^{(\hat{k},k)} \left(\mathbf{P}_m^{(\hat{k},k)} \right)^H$ that does not depend on the time index m .

Now, we define $\mathbf{R}_{\text{SINR}}^{(k)}$ as the sum of the correlation matrices of the interference (ISI, ICI, and MAI) and the noise; that is,

$$\mathbf{R}_{\text{SINR}}^{(k)} = \mathbf{R}_{\text{ISI}}^{(k)} + \mathbf{R}_{\text{ICI+MAI}}^{(k)} + \mathbf{R}_\eta^{(k)}. \quad (\text{A.7})$$

If we compute the Cholesky factorization of the correlation matrix [15], that is, $\mathbf{R}_{\text{SINR}}^{(k)} = \mathbf{D}\mathbf{D}^H$, and we define the vector $\mathbf{u} = \mathbf{D}^{-1}\mathbf{p}_d^{(k)}$, we can rewrite (A.6) as

$$\text{SINR}^{(k)} = \frac{\left| \mathbf{u}^H \mathbf{D}^H \mathbf{w}_{\text{SINR}}^{(k)} \right|^2}{\left(\mathbf{D}^H \mathbf{w}_{\text{SINR}}^{(k)} \right)^H \left(\mathbf{D}^H \mathbf{w}_{\text{SINR}}^{(k)} \right)}. \quad (\text{A.8})$$

Using the Cauchy-Schwarz inequality [15] the SINR is maximum when $\mathbf{u} \propto \mathbf{D}^H \mathbf{w}_{\text{SINR}}^{(k)}$, and it is equal to $\text{SINR}^{(k)} = \mathbf{u}^H \mathbf{u}$.

Equating the relations $\mathbf{u} = \mathbf{D}^{-1}\mathbf{p}_d^{(k)}$ and $\mathbf{u} = \mathbf{D}^H \mathbf{w}_{\text{SINR}}^{(k)}$, we obtain the optimum solution for the equalizer coefficients that is given by

$$\mathbf{w}_{\text{SINR}}^{(k)} = \left(\mathbf{D}\mathbf{D}^H \right)^{-1} \mathbf{p}_d^{(k)} = \left(\mathbf{R}_{\text{SINR}}^{(k)} \right)^{-1} \mathbf{p}_d^{(k)}. \quad (\text{A.9})$$

Finally, the maximum SINR at the equalizer output is equal to

$$\text{SINR}_{\text{MAX}}^{(k)} = \mathbf{u}^H \mathbf{u} = \left(\mathbf{p}_d^{(k)} \right)^H \left(\mathbf{R}_{\text{SINR}}^{(k)} \right)^{-1} \mathbf{p}_d^{(k)}. \quad (\text{A.10})$$

A.2. Relation between the Maximum SINR and the MMSE Equalizer. The MMSE equalizer [13] minimizes the error between its output and the data symbol of interest $a_{m-d}^{(k)}$; that is, $\varepsilon_m = \hat{a}_m^{(k)} - a_{m-d}^{(k)}$, where d is a certain delay, by minimizing the quadratic form $J = E[\varepsilon_m \varepsilon_m^*]$. The optimum vector $\mathbf{w}_{\text{MMSE}}^{(k)}$ is obtained from the orthogonality condition $E[\varepsilon_m (\mathbf{z}_m^{(k)})^H] = \mathbf{0}$ that corresponds to the following relation:

$$\left(\mathbf{w}_{\text{MMSE}}^{(k)} \right)^H E \left[\mathbf{z}_m^{(k)} \left(\mathbf{z}_m^{(k)} \right)^H \right] = E \left[a_{m-d}^{(k)} \left(\mathbf{z}_m^{(k)} \right)^H \right]. \quad (\text{A.11})$$

The correlation matrix of the input is given by

$$\mathbf{R}_{\text{MMSE}}^{(k)} = E \left[\mathbf{z}_m^{(k)} \left(\mathbf{z}_m^{(k)} \right)^H \right] = \sum_{\hat{k}=0}^{M-1} \mathbf{P}_m^{(\hat{k},k)} \left(\mathbf{P}_m^{(\hat{k},k)} \right)^H + \mathbf{R}_\eta^{(k)}, \quad (\text{A.12})$$

while

$$E \left[a_{m-d}^{(k)} \left(\mathbf{z}_m^{(k)} \right)^H \right] = \left(\mathbf{p}_d^{(k)} \right)^H. \quad (\text{A.13})$$

Substituting (A.12) and (A.13) in (A.11), we obtain

$$\mathbf{w}_{\text{MMSE}}^{(k)} = \left(\mathbf{R}_{\text{MMSE}}^{(k)} \right)^{-1} \mathbf{p}_d^{(k)}. \quad (\text{A.14})$$

Generalizing the results in [13] to take into account the presence of ICI and MAI, the SINR at the output of the MMSE equalizer is equal to

$$\text{SINR}_{\text{MMSE}}^{(k)} = \frac{\left(\mathbf{p}_d^{(k)} \right)^H \left(\mathbf{R}_{\text{MMSE}}^{(k)} \right)^{-1} \mathbf{p}_d^{(k)}}{1 - \left(\mathbf{p}_d^{(k)} \right)^H \left(\mathbf{R}_{\text{MMSE}}^{(k)} \right)^{-1} \mathbf{p}_d^{(k)}}. \quad (\text{A.15})$$

To prove the equivalence between the MMSE and the maximum SINR equalizer we use the relation

$$\mathbf{R}_{\text{SINR}}^{(k)} = \mathbf{R}_{\text{MMSE}}^{(k)} - \mathbf{p}_d^{(k)} \left(\mathbf{p}_d^{(k)} \right)^H. \quad (\text{A.16})$$

For the matrix inversion identity [16] we have

$$\begin{aligned}
 & \left(\mathbf{R}_{\text{MMSE}}^{(k)} - \mathbf{P}_d^{(k)} \left(\mathbf{P}_d^{(k)} \right)^H \right)^{-1} \\
 &= \left(\mathbf{R}_{\text{MMSE}}^{(k)} \right)^{-1} \\
 &+ \frac{\left(\mathbf{R}_{\text{MMSE}}^{(k)} \right)^{-1} \mathbf{P}_d^{(k)} \left(\mathbf{P}_d^{(k)} \right)^H \left(\mathbf{R}_{\text{MMSE}}^{(k)} \right)^{-1}}{1 - \left(\mathbf{P}_d^{(k)} \right)^H \left(\mathbf{R}_{\text{MMSE}}^{(k)} \right)^{-1} \mathbf{P}_d^{(k)}} \quad (\text{A.17}) \\
 &= \left(\mathbf{R}_{\text{SINR}}^{(k)} \right)^{-1}.
 \end{aligned}$$

Substituting (A.17) in (A.10) we can write

$$\begin{aligned}
 & \text{SINR}_{\text{MAX}}^{(k)} \\
 &= \left(\mathbf{P}_d^{(k)} \right)^H \left(\mathbf{R}_{\text{MMSE}}^{(k)} \right)^{-1} \mathbf{P}_d^{(k)} \\
 &+ \frac{\left(\mathbf{P}_d^{(k)} \right)^H \left(\mathbf{R}_{\text{MMSE}}^{(k)} \right)^{-1} \mathbf{P}_d^{(k)} \left(\mathbf{P}_d^{(k)} \right)^H \left(\mathbf{R}_{\text{MMSE}}^{(k)} \right)^{-1} \mathbf{P}_d^{(k)}}{1 - \left(\mathbf{P}_d^{(k)} \right)^H \left(\mathbf{R}_{\text{MMSE}}^{(k)} \right)^{-1} \mathbf{P}_d^{(k)}} \\
 &= \frac{\left(\mathbf{P}_d^{(k)} \right)^H \left(\mathbf{R}_{\text{MMSE}}^{(k)} \right)^{-1} \mathbf{P}_d^{(k)}}{1 - \left(\mathbf{P}_d^{(k)} \right)^H \left(\mathbf{R}_{\text{MMSE}}^{(k)} \right)^{-1} \mathbf{P}_d^{(k)}} \\
 &= \text{SINR}_{\text{MMSE}}^{(k)}, \quad (\text{A.18})
 \end{aligned}$$

which proves that the SINR at the MMSE equalizer output is identical to the SINR at the maximum SINR equalizer output. Furthermore, the vectors $\mathbf{w}_{\text{SINR}}^{(k)}$ and $\mathbf{w}_{\text{MMSE}}^{(k)}$ differ by a constant factor as proved below:

$$\begin{aligned}
 \mathbf{w}_{\text{SINR}}^{(k)} &= \left(\mathbf{R}_{\text{MMSE}}^{(k)} \right)^{-1} \mathbf{P}_d^{(k)} \\
 &+ \frac{\left(\mathbf{R}_{\text{MMSE}}^{(k)} \right)^{-1} \mathbf{P}_d^{(k)} \left(\mathbf{P}_d^{(k)} \right)^H \left(\mathbf{R}_{\text{MMSE}}^{(k)} \right)^{-1} \mathbf{P}_d^{(k)}}{1 - \left(\mathbf{P}_d^{(k)} \right)^H \left(\mathbf{R}_{\text{MMSE}}^{(k)} \right)^{-1} \mathbf{P}_d^{(k)}} \quad (\text{A.19}) \\
 &= \mathbf{w}_{\text{MMSE}}^{(k)} \left(1 + \text{SINR}_{\text{MMSE}}^{(k)} \right).
 \end{aligned}$$

Acknowledgments

The work of this paper has been partially supported by the European Community Seventh Framework Programme FP7/2007–2013 under Grant agreement no. 213311, project OMEGA-Home Gigabit Networks. The authors wish to thank the anonymous reviewers whose comments helped to improve the clarity of this paper.

References

- [1] A. M. Tonello, "Asynchronous multicarrier multiple access: optimal and sub-optimal detection and decoding," *Bell Labs Technical Journal*, vol. 7, no. 3, pp. 191–217, 2003.
- [2] S. Weinstein and P. Ebert, "Data transmission by frequency-division multiplexing using the discrete Fourier transform,"

- IEEE Transactions on Communications*, vol. 19, no. 5, pp. 628–634, 1971.
- [3] G. Cherubini, E. Eleftheriou, and S. Ölçer, "Filtered multitone modulation for very high-speed digital subscriber lines," *IEEE Journal on Selected Areas in Communications*, vol. 20, no. 5, pp. 1016–1028, 2002.
- [4] A. M. Tonello, "Time domain and frequency domain implementations of FMT modulation architectures," in *Proceedings of IEEE International Conference on Acoustics, Speech and Signal Processing (ICASSP '06)*, vol. 4, pp. 625–628, Toulouse, France, May 2006.
- [5] T. M. Schmidl and D. C. Cox, "Robust frequency and timing synchronization for OFDM," *IEEE Transactions on Communications*, vol. 45, no. 12, pp. 1613–1621, 1997.
- [6] S. Kaiser and W. A. Krzymien, "Performance effects of the uplink asynchronism in a spread spectrum multi-carrier multiple access system," *European Transactions on Telecommunications*, vol. 10, no. 4, pp. 399–406, 1999.
- [7] J.-J. van de Beek, P. O. Börjesson, M.-L. Boucheret et al., "Time and frequency synchronization scheme for multiuser OFDM," *IEEE Journal on Selected Areas in Communications*, vol. 17, no. 11, pp. 1900–1914, 1999.
- [8] A. M. Tonello, N. Laurenti, and S. Pupolin, "Analysis of the uplink of an asynchronous multi-user DMT OFDMA system impaired by time offsets, frequency offsets, and multipath fading," in *Proceedings of the 52nd Vehicular Technology Conference (VTC '00)*, pp. 1094–1099, Boston, Mass, USA, September 2000.
- [9] J. Choi, C. Lee, H. W. Jung, and Y. H. Lee, "Carrier frequency offset compensation for uplink of OFDM-FDMA systems," *IEEE Communications Letters*, vol. 4, no. 12, pp. 414–416, 2000.
- [10] Z. Cao, U. Tureli, and Y.-D. Yao, "Deterministic multiuser carrier-frequency offset estimation for interleaved OFDMA uplink," *IEEE Transactions on Communications*, vol. 52, no. 9, pp. 1585–1594, 2004.
- [11] V. Lottici, M. Luise, C. Saccomando, and F. Spalla, "Non-data-aided timing recovery for filter-bank multicarrier wireless communications," *IEEE Transactions on Signal Processing*, vol. 54, no. 11, pp. 4365–4375, 2006.
- [12] A. M. Tonello and F. Pecile, "Synchronization algorithms and receiver structures for multiuser filter bank uplink systems," *EURASIP Journal on Wireless Communications and Networking*, vol. 2009, Article ID 387520, 17 pages, 2009.
- [13] J. G. Proakis, *Digital Communications*, McGraw-Hill, New York, NY, USA, 3rd edition, 1995.
- [14] S.-W. Hou and C. C. Ko, "Multiple-access interference suppression for interleaved OFDMA system uplink," *IEEE Transactions on Vehicular Technology*, vol. 57, no. 1, pp. 194–205, 2008.
- [15] R. A. Horn and C. R. Johnson, *Matrix Analysis*, Cambridge University Press, New York, NY, USA, 1990.
- [16] M. Brookes, "The Matrix Reference Manual," 2005, <http://www.ee.ic.ac.uk/hp/staff/dmb/matrix/intro.html>.